Chemometrics and Intelligent Laboratory Systems 157 (2016) 1–6

Contents lists available at ScienceDirect

Chemometrics and Intelligent Laboratory Systems

journal homepage: www.elsevier.com/locate/chemolab

A new algorithm for lane detection and tracking on pulsed field gel electrophoresis images

Mohammad Rezaei [a], Mahmood Amiri [b,*], Parviz Mohajeri [c], Mansour Rezaei [d]

[a] Students Research Committee, Kermanshah University of Medical Sciences, Kermanshah, Iran
[b] Medical Biology Research Center, Kermanshah University of Medical Sciences, Kermanshah, Iran
[c] Department of Microbiology, School of Medicine, Kermanshah University of Medical Sciences, Kermanshah, Iran
[d] Department of Biostatistics, Social Development & Health Promotion Research Center, Kermanshah University of Medical Sciences, Kermanshah, Iran

ARTICLE INFO

Article history:
Received 20 July 2015
Received in revised form 21 May 2016
Accepted 27 May 2016
Available online 28 May 2016

Keywords:
Lane detection
PFGE image
Power spectrum density

ABSTRACT

In this paper, a new method is presented for lane detection and extraction on the pulsed field gel electrophoresis (PFGE) images. Average lane width and lane curvature are the most important parameters that are required for automatic image processing of PFGE images. For this purpose, a new algorithm based on computing the power spectrum density (PSD) is proposed for automatic lane detection and tracking. The PSD is used to calculate the average lane width and then partitioning original images to sub-images, tolerating some overlaps. The performance of the proposed algorithm has been evaluated on 30 PFGE images which totally form 300 lanes. Results show that the new algorithm has better performance in lane width detection compared to the other methods such as intersection of the horizontal lines and reaches 99.66%. Finally, it can also be used as a software tool for automatic analysis of PFGE images.

1. Introduction

Standard gel electrophoresis methods for separation of Deoxyribonucleic acid (DNA) molecules provide several advantages for molecular biology researches. However, it is not able to separate very large molecules of DNA, effectively. To overcome this problem, a technique was developed in 1984, in which the large parts of DNA can be separated by changing the direction of the electric current and it is currently known as Pulsed-Field Gel Electrophoresis (PFGE). PFGE is one of the common methods for molecular typing and epidemiological studies [1].

PFGE images contain several vertical stripes called *lane*. Each lane consists of a group of DNA fragments which form the horizontal bands, having nearly constant width [2]. The advent of digital image technology provided a direct method for creating gel electrophoresis images in a specific format for forthcoming analysis [3]. Digital gel electrophoresis images are widely used to extract valuable information from biological materials in various molecular biology applications [4]. For example, it is used to find the relationship between an unknown biological specimen and a known biological one by comparing their DNA patterns [2]. On the other hand, manual analyzing and evaluation of images is not only a boring task but also it probably rises human errors [5,6].

Today, analysis and processing of these images such as lane extraction and band localizing are carried out by computers [3]. Different factors including electrical charge of particles, temperature and pH of the surrounding environment affect the quality of the produced images which give rise to the process of lane extraction and band localizing to be more difficult. It should be pointed out that the main purpose of the image analysis is to properly detect bands and then to compare the lanes using the obtained band location. Consequently, in the first step the lanes should be correctly extracted and then individual lane be prepared for future analysis.

Since PFGE and Polymerase Chain Reaction (PCR) images have similar characteristics, it is helpful to use the studies which were conducted on PCR images. Therefore, several methods were suggested to solve the problem of visual analysis which was time consuming and inaccurate [7]. The first step in processing of PFGE images is lane extraction which is also called lane tracking [8]. Because the accuracy of band detection depends on the accuracy of lane detection, it is necessary to apply techniques for better lane detection. Akbari and his colleagues presented, a semi-automatic method for lane detection [7]. In their proposed method, the number of lanes in the image must be entered manually by the user. Meanwhile, a commercial software is also designed [3]. By determining the number of lanes, their average width can be estimated which is a very important factor for the succeeding steps of lane detection such as smoothing signal, removing the undesirable centers or connecting the desirable lane centers in all of the sub-images. Most semi-automatic and automatic methods proposed for lane detection are based on the visual

* Corresponding author at: Parastar Ave., Kermanshah University of Medical Sciences, Kermanshah, Iran. Tel: +988338237033.
E-mail address: ma.amiri@ece.ut.ac.ir (M. Amiri).

http://dx.doi.org/10.1016/j.chemolab.2016.05.018
0169-7439/

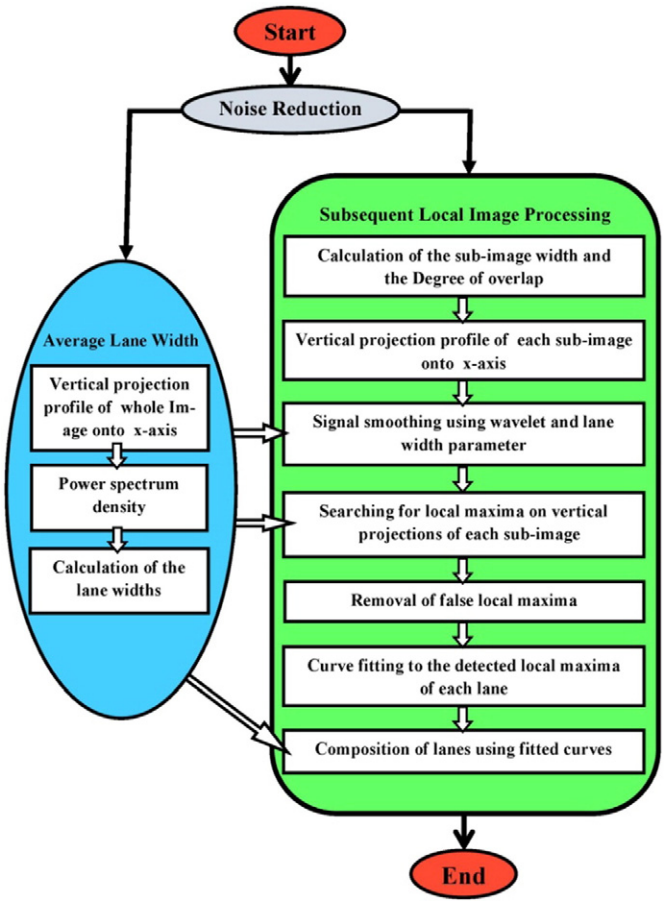

Fig. 1. The flowchart of the proposed algorithm.

projection profile (VPP) onto the x-axis [9]. To smooth the signals from the VPP, the wavelet transform can be used [10]. Furthermore, for choosing the appropriate parameters of wavelet, it is necessary to use the average width of individual lane.

One common method to estimate the lane average width is to intersect a horizontal line with the signal obtained from the VPP and then find the distance from the sequential cut-off points as the lane width and finally calculate the average value of all lane widths. This procedure

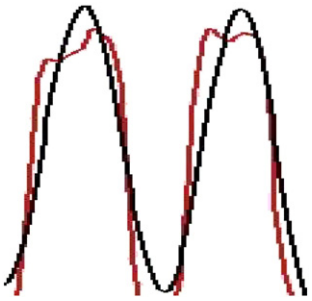

Fig. 3. Black signal is the result of the smoothing of red signal. As it can be seen, undesirable local maxima have been removed.

is called intersection horizontal line (IHL) [11]. Clearly, the aforementioned method is not an accurate estimation of the lane average width. Therefore, in the current research, a new method based on power spectral density of the VPP is proposed to calculate the average width of the lane in PFGE images. In this case, the VPP is acquired for the whole PFGE image and then power spectrum density of the signal is computed. It will be shown that the second frequency which has the higher amplitude could be considered as the value corresponding to the average width of the lane.

Another challenge in the process of lane tracking is the lane curvature. In [11], a new method was developed to solve this challenge. They were able to approximately detect the curvature of lane by partitioning individual image into N sub-images along x-axis. Nevertheless, there was a limitation on the number of sub-images. Indeed, partitioning the original image into more sub-images leads to the better detection of the lane curvature. However, it increases the amount of noise which can cause incorrect detection of lane centers in each sub-image. This is due to the reduced width of sub-images. Consequently, in this paper, to overcome this limitation, partitioning of the original images into sub-images is performed by allowing some overlaps between sub-images.

The rest of paper is organized as follows: Section 2 describes data set, the proposed method for lane tracking, including image preprocessing steps, calculating the lane average width based on power spectral density and partitioning the original image. Results and Discussion are explained in Sections 3 and 4, respectively and finally, Section 5 concludes the paper.

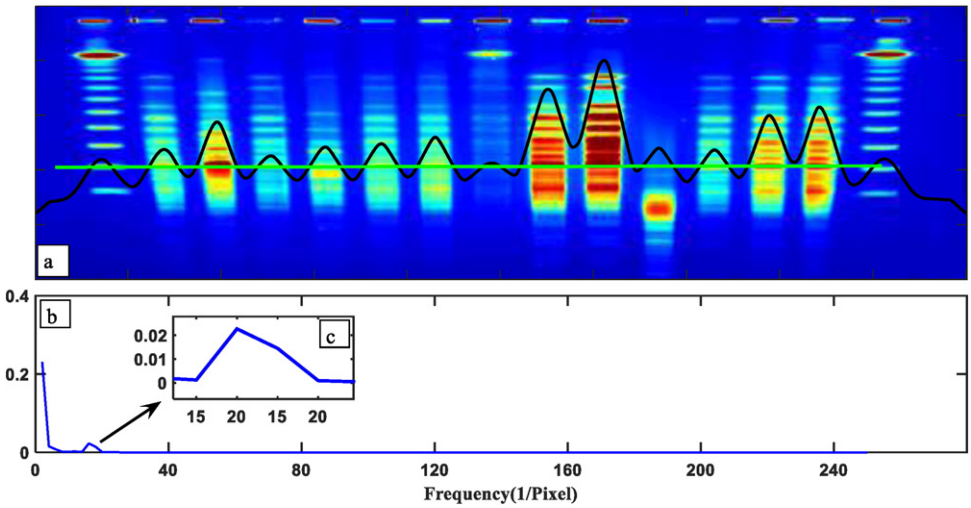

Fig. 2. Calculating the average lane width using PSD: (a) an example of typical PFGE images. (b) Corresponding power spectrum density graph. (c) The magnified portion of (b) in which the second peak has inverse relationship with the average lane width.

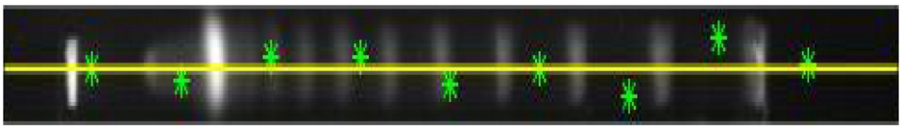

Fig. 4. Example of curve fitting on detected centers (green stars) and the obtained curve (yellow curve).

2. Materials and methods

2.1. Material

In this research, 30 PFGE images, containing 450 lanes, were used. All images were provided by PFGE BIORAD model in Microbiology Laboratory of Kermanshah University of Medical Sciences. Images are provided by three types of bacteria, including Acineto-AF and *Staphylococcus aureus* and *E. coli*. All images are in .tif format and have 500 × 500 pixels of size. The number of lanes per image varies from 14 to 18. 10 images were used as training data set and 20 images were utilized for test data set randomly. All designed algorithms were implemented and carried out in MATLAB environment version R2009a. Moreover, the software GelCompar II version 6.6.11 in trial version was used to evaluate the algorithms.

2.2. Methods

The proposed lane detection algorithm is composed of two stages including calculation of the average lane width and subsequent local image processing. The flowchart of the proposed method is shown in Fig. 1. In the first step, all images are converted into gray scale images and then resized by 500∗500 pixels. The average lane width is estimated by computing the power spectrum density of the VPP signal acquired from the whole input image. Next, the whole image is partitioned into several sub-images for subsequent local image processing to track the centers and detect the partitioned lanes. In previous methods, to obtain sub-images, no overlap was allowed [11]. However, in this paper, sub-images were selected with some overlap between neighboring sub-images. It should be emphasized, before carrying out each stage, that a high-speed non-linear adaptive median filter was applied to individual gel electrophoresis images to remove the noise generated during PFGE image acquisition [12–14]. Impulsive noise is reduced with a series of median filters nevertheless other methods could also be used. In this study, wavelet transform was also used. By selecting the optimal parameters, the same results were obtained.

2.2.1. Computing the lane average width

The power spectrum density (PSD) estimation is used to estimate the power of frequency components of a signal [15]. Vertical projection profile is a transformation from 2-D information of the image to 1-D information while the intensities (values) of the pixels in each column of the image are accumulated [11]. In this way, projection profile was obtained from original images on x-axis. Here, the PSD of the VPP signal can be obtained as illustrated in Fig. 2. Results show that the power spectrum of this signal is much denser around a specific frequency which in turn specifies the frequency of lane repetition. In PFGE images, as shown in Fig. 2 (a), the amplitude of the projection profile signal calculated along a lane is higher than the amplitude between two lanes. This is due to the fact that each lane is composed of a sparsely located horizontal bands which are relatively brighter than the background [16,17]. It should be pointed out that the PSD is not indicating the lane width and it actually measures the inter-lane distance. However, in all lane widths, a direct relation with inter-lane space exists and indeed, it has a little bit smaller and in this study it was approximately 0.85% of the inter-lane space.

As shown in Fig. 2 (b), the PSD has two obvious peaks. The first peak is related to the background activity and the second peak reflects the

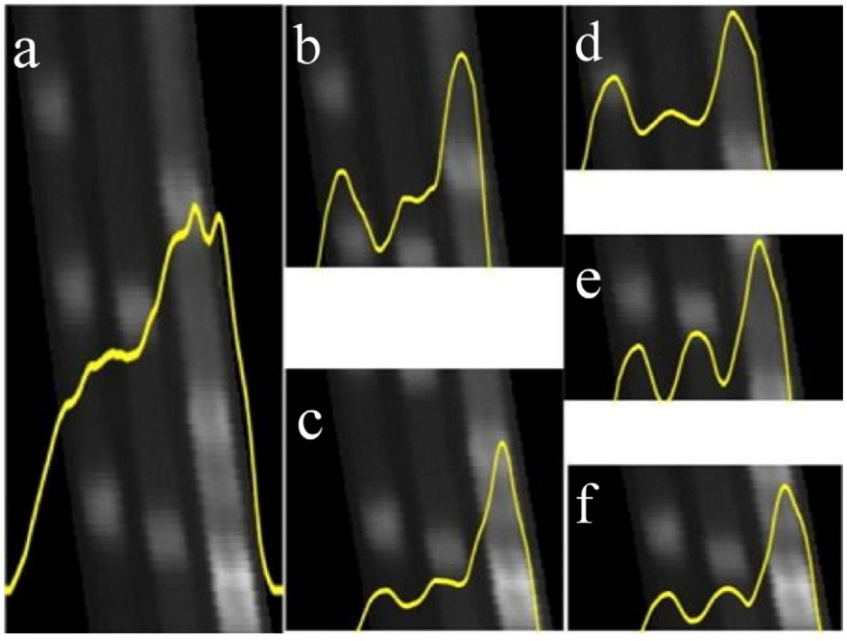

Fig. 5. (a) Three "curved" lanes. (b), (c) image segmentation into two sub-images. (d)–(f) Image segmentation into three sub-images. Increasing the number of sub-images reduces the "curvature effect".

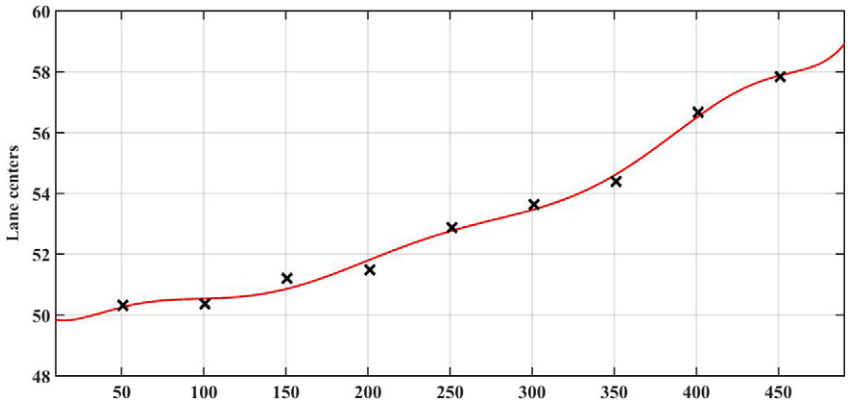

Fig. 6. Detected centers in a lane and its fitted curve. The crosses are detected centers and then a curve has been fitted using conic spline method.

lane width (Fig. 2 (c)). As the lane width decreases, the frequency of the second peak increases. Therefore, the lane width has an inverse relationship with the detected frequency as described in Eq. (1).

$$w = \frac{1}{f} * (\text{length of projection profiles}) \tag{1}$$

where w is the width of lane and f is related frequency. Inter-lane distance can slightly effect on VPP signal but is negligible because PSD procedure calculates not lane width, but inter-lane distance.

2.2.2. Local image processing techniques

After determining the lane width, the local image processing techniques are applied. Initially, width and percentage of overlaps of sub-images are determined. Second, the algorithm finds the local maxima on vertical projection signal calculated for each partitioned image using the second derivative test. The algorithm is capable of detecting peaks within the specified width and slope to avoid detection of false local maxima. Indeed, if the difference between local maxima and average width of lane increases, they are not detected. False local maxima are detected in few steps and then removed. In preprocessing step, some of them are removed by smoothing the VPP signal. For optimum smoothing, the average width of the lane was used. As Fig. 3 shows, if the distance of two local maxima was less than half average width of lane, it indicates that they are on the same lane and one of them is undesirable and hence it will be removed from subsequent calculations.

Next, lane centers located in the same vertical position are identified. Finally, the path of each lane is tracked by curve fitting of detected centers for each lane. Curve fitting reduces the detection error of center of lane. For curve fitting, conic spline is used. Fig. 4 indicates this case.

2.2.3. Partitioning input images

Selecting the optimum number of sub-images can affect lane detection. In [11], the best results were obtained by partitioning the original image into 10 sub-images. As previously mentioned, if the image is partitioned into more sub-images, the lane curvature can be detected straightforward. By increasing the width of sub-images, it is easier to remove undesirable local maxima. However, when the lane is curved "enough", we must reduce the width of sub-images in order to reduce the curvature effect. As seen in Fig. 5, when the image is partitioned in three parts (Fig. 5 (d)–(f)), the local maxima were better detected.

The challenge is that if the image is partitioned into more sub-images, the effect of noise increases. On the other hand, image partitioning into lower sub-images leads to incorrect detection of the lane. For example, if a white spot noise exists in each sub-image, it appears on VPP signal as a local maximum and consequently it causes miscalculation. In [11], the image was partitioned into 10 sub-images so that the width of each sub-image is 50 pixels. However, according to the method proposed in this paper, if 75 pixels are considered for the sub-image width and 50 pixels for the amount of overlap, not only the sub-image width increases 50%, but also their numbers have increased to 180% of the non-overlapping condition.

2.2.4. Lane detection in sub-images

At this stage, the lanes' centers are acquired in all sub-images. Indeed, the VPP signal of each sub-image is preprocessed using wavelet transform [18]. Then the centers of lanes are calculated. In this paper,

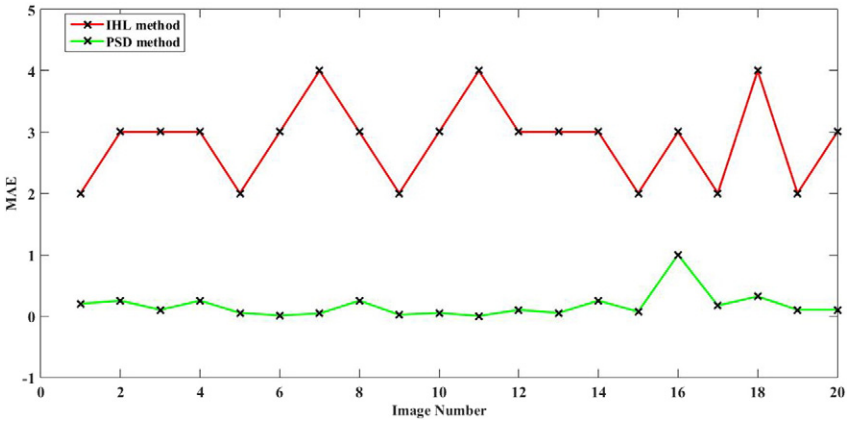

Fig. 7. The MAE of average lane width obtained from applying PSD and IHL methods on VPP signal for 20 test images.

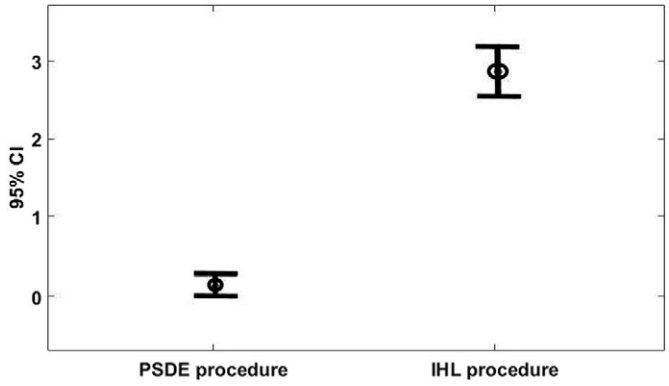

Fig. 8. Error bar charts of average lane width detection process for PSD and IHL procedures with actual values. The corresponding 95% confidence interval (CI) for PSD and IHL techniques.

we investigated which particular wavelet would achieve the best performance considering the smoothing and baseline drift removal. We considered some of the most available wavelets in MATLAB: Daubechies wavelets db2 to db45, Biorthogonal wavelets bior1.1 to bior6.8, Reverse Biorthogonal wavelets rbior1.1 to rbior6.8, Symlets wavelets sym2 to sym36, and Coiflets wavelets coif1 to coif5. We have also varied the decomposition level from 4 to 12. Finally, Daubechies wavelet db7 by decomposition level 6 was selected. It should be noted, that the average lane width was also used to select the type of wavelet. Finally, lane centers that are located in the same vertical position are identified. Then, lane path is tracked by curve fitting of the detected centers of each lane as shown in Fig. 6. The average lane width was used to remove false positive local maxima in background. Note that the average lane width and curve fitting of detected centers within each lane lead to the increase of the efficiency for lane extraction process. It should be pointed out that both cubic and conic splines perform well when the lane centers are detected with high precision. For low precision detection of lane centers, the conic spline has better performance.

3. Results

The evaluation of the proposed algorithm was conducted in two stages: First, we evaluated its performance on calculation of the average lane width. Next, the process of lane detection was assessed. Fig. 7 shows the error for the average lane width detection obtained by PSD and IHL methods. In both cases, the average width of the lanes for all images was calculated and compared with the actual values. To compute the error, the mean absolute error (MAE) was used [19]. As Fig. 7 illustrates, the proposed algorithm performs quite well for all 20 test images and yields low MAE compared to the IHL method.

The result of ANOVA is shown in Fig. 8. In this way, it is evident that the average lane width obtained from the IHL procedure relative to the actual values has a significant difference ($P-value<0.0001$). On the other hand, it has no significant difference with actual values for PSD method ($P-value=0.862$). Also, 95% confidence interval (CI) is [2.54, 3.16] for IHL technique and is [0.12, 0.14] for PSD method.

Table 1
Performance of the lane detection algorithm using various combinations of the width and amount of overlaps between sub-images.

Overlap (in pixel)	Width the sub-image (in pixel)			
	75s	100	125	150
25	99.02%	99.96%	100%	98.25%
50	99.86%	100%	100%	100%
75	99.95%	99.98%	100%	100%

Table 2
Comparison with the other methods.

Method	Results			
	t_p	f_p	f_n	F-measure
Akbari et al. [7]	243	45	12	89.5%
Sousa et al. [9]	275	18	7	95.65%
Park et al. [11]	281	13	6	96.73%
Proposed	298	2	0	99.66%

Overall, considering that the MAE is 2.85 in the IHL procedure and 0.01 in PSD procedure, it is observed that the proposed algorithm reduces more than 99.61% of IHL error. To train total algorithm of lane detection, 10 PFGE images with 30 different conditions for width and percentage of sub-images overlap were used. At each training phase, precision and recall were calculated to obtain F-measure and to quantify the performance of the detection scheme. Similar to [20], the F-measure is defined as:

$$\text{F-measure} = \frac{1}{1+\left(f_p+f_n\right)/2t_p} \tag{2}$$

where t_p, f_p and f_n are true positive, false positive, and false negative, respectively. Finally, 12 different conditions were selected. In the test phase, we also calculated F-measure to evaluate the performance of the proposed algorithm optimized with effective parameters. Table 1 shows the results of the test phase. The worst F-measure was 98.25% and the best F-measure was 100% that includes 5 conditions. Regarding computational time, the fastest response is obtained about 0.761 s for an image with MATLAB R2009a and personal computer (PC) equipped with Intel_Core™ i5 2.4 GHz CPU and 4 GB RAM. Thus, considering computational cost and good performance, the optimal parameters for width and sub-image overlap are 100 and 50 pixels, respectively.

4. Discussion

Nowadays, computers are widely used for various processing procedures at different stages of PFGE image analysis. Lane detection and extraction is the first step of PFGE image processing and analysis. The accuracy of all subsequent analysis depends on the accuracy and precision of this stage. So far the most popular method for lane detection is using the projection profile onto x and y axes [7,9]. Since the experimental conditions such as temperature, pH and even electric charge of particles can affect quality of PFGE images and lead to have curved lanes, a new algorithm was proposed and tested for detection and extraction of curved lanes. Our proposed algorithm has several unique features mentioned below.

According to widespread application of wavelet, in this study, we used it for signal smoothing [21–23]. For this purpose, the average lane width was used to select the optimal parameters of the wavelet transform. Akbari and colleagues in [7] used averaging method for smoothing and Sousa and collaborators in [9] utilized average width of lane parameter to select the appropriate window for smoothing. At this stage, this parameter is very important and if it is obtained with error, some of desired local maxima cannot be detected properly. Because the lane center on each sub-image corresponds to the local maxima, their false detection leads to incorrect lane detection.

To calculate the average width of the lane, the intersection of the horizontal line parallel to the x-axis with the projection profile signal was used in [11]. Despite applying the horizontal line method in the most common coordination system and its simplicity, the actual widths of some lanes are calculated with high error. This is due to unequal height of peaks and hence no intersections of the horizontal line with full width at half maximum (FWHM) have happened. In our proposed

algorithm, the PSD technique was used. Since the second highest amplitude in the power spectrum in frequency domain corresponds to the average lane width, detection of this frequency provides a good estimation of the average lane width. In this way, the MAE significantly reduced and the performance increased up to 99.61%. In addition to smoothing the signal, the average lane width was also used for removing the false local maxima and finding the lane centers on a specific lane. Therefore, the method increases the performance of the proposed algorithm.

Another feature of our proposed algorithm is partitioning the image into sub-images with overlap. Sousa and colleagues partitioned the image into sub-images without overlaps to detect the lane curvature but it limits the number of sub-images [11]. The nature of the VPP signal is such that the number of sub-images cannot be considered more or less and it affects the algorithm performance. Two factors must be taken into account to be able to detect the lane ideally. Indeed, increasing the width of sub-images leads to the increase of signal to noise ratio (SNR) which in turn decreases the detected false local maxima. Moreover, the large number of sub-images can result in better detection of lane curvature. Therefore, these factors should be carefully selected. Considering the overlap can overcome the existing restrictions and more sub-images without reduced width is obtained. In our study, several conditions were considered to obtain the optimum width of sub-images and overlapping level and the best result was obtained with 100 and 50 pixels for them, respectively. It should be noted that, big overlap of sub-images has two disadvantages. First, it increases the computation time. Although it helps to better detect the lane curvature, but if there is significant error, it's likely to increase. Therefore it is recommended to avoid excessive increase in overlap. The results indicated that when overlap was more than two-thirds of the width of the sub-images, then the error increases as illustrated in Table 1. In this study, we focused on improving the detection of curved lanes in PFGE images. The PSD method was used to calculate the average width of the lane and sub-images with some overlaps to solve challenges in Ref [1]. Moreover, Refs. 7, 8, 9 and 16 were not focused on the curved lanes.

Curve fitting of each lane is the other issue which was investigated in this study. Even assuming that all the lane centers are detected properly, existence of error and little difference in detection of actual centers is possible. This can be seen in Fig. 6. Using curve fitting reduces the error and it can also be used to facilitate the separation of lanes from original image. Big overlap of sub-images has two disadvantages. First, it increases the processing time. Although it helps to better detect the lane curvature, but if there is an error, it's likely to increase. Therefore it is recommended to avoid excessive increase overlap. The results indicated that when the amount of overlap is more than two-thirds the width of the sub-images, the error increases.

Finally, the proposed algorithm was compared with the other methods reported in [7,9,11]. The results were reported in Table 2. As this table shows, the new algorithm has better performance. It should be pointed out that the results in Table 2 were obtained for images with low lane curvature. For large lane curvature, the proposed algorithm is significantly superior to compared methods.

5. Conclusion

In this paper, we proposed an automatic approach for lane detection and extraction in PFGE images. This approach mainly consists of calculating average width of lanes using PSD procedure and lane segmentation and optimal line fitting to separate lanes. Experimental results showed that PSD procedure compared with other procedures has good performance with small error. In this way, partitioning the image into several sub-images with some overlaps and then using curve fitting to separate lanes reduce lane detection errors. Experimental results showed that the proposed lane segmentation algorithm is robust to low-contrast, spot-noise and slant lanes. Considering that lane detection is important as a first step in analysis of PFGE images, the proposed algorithm can also be used for lane extraction. Future works will be conducted to use artificial intelligence and artificial neural networks [24–26] and adapt the approach to deal with other types of electrophoresis images such as PCR, PAGE, FIGE images.

Acknowledgment

The authors gratefully acknowledge the Research Council of Kermanshah University of Medical Sciences for the financial support.

The authors would like to thank the anonymous and esteemed reviewers for their valuable and insightful comments on the earlier drafts of this paper.

References

[1] B. Birren, E. Lai, Pulsed Field Gel Electrophoresis: a Practical Guide, Academic Press, 2012.
[2] A.R. Hoelzel, G.A. Dover, Molecular Genetic Ecology, IRL Press at Oxford University Press, 1991.
[3] J. Pizzonia, Product application focus electrophoresis gel image processing and analysis using the KODAK 1D software, Biotechniques 30 (6) (2001) 1316–1320.
[4] Efficient quantitative information extraction from PCR-RFLP gel electrophoresis images, in: C. Maramis, A. Delopoulos (Eds.), Proceedings of the 2010 20th International Conference on Pattern Recognition, IEEE Computer Society, 2010.
[5] A. Blatter, E. Reich, Qualitative and quantitative HPTLC methods for quality control of *Stephania tetrandra*, J. Liq. Chromatogr. Relat. Technol. 27 (13) (2005) 2087–2100.
[6] A. Schibli, E. Reich, Modern TLC: a key technique for identification and quality control of botanicals and dietary supplements, JPC J. Planar Chromatogr. - Mod. TLC 18 (101) (2005) 34–38.
[7] A. Akbari, F. Albregtsen, K.S. Jakobsen, Automatic lane detection and separation in one dimensional gel images using continuous wavelet transform, Anal. Methods 2 (9) (2010) 1360–1371.
[8] R.T. Wong, S. Flibotte, R. Corbett, P. Saeedi, S.J. Jones, M.A. Marra, et al., LaneRuler: automated lane tracking for DNA electrophoresis gel images, IEEE Trans. Autom. Sci. Eng. 7 (3) (2010) 706–708.
[9] A.V. Sousa, R. Aguiar, A.M. Mendonça, A. Campilho, Automatic lane and band detection in images of thin layer chromatography, Image Analysis and Recognition, Springer 2004, pp. 158–165.
[10] An iterative algorithm for segmenting lanes in gel electrophoresis images, in: M. AM, C. MF, S. AM, D.C. OS (Eds.), Computer Graphics and Image Processing, 1997 Proceedings, X Brazilian Symposium on, IEEE, 1997.
[11] S.C. Park, I.S. Na, T.H. Han, S.H. Kim, G.S. Lee, Lane detection and tracking in PCR gel electrophoresis images, Comput. Electron. Agric. 83 (2012) 85–91.
[12] D. Dhanasekaran, K.B. Bagan, High speed pipelined architecture for adaptive median filter, Eur. J. Sci. Res. 29 (4) (2009) 454–460.
[13] K. Kaczmarek, B. Walczak, S. de Jong, B.G. Vandeginste, Preprocessing of two-dimensional gel electrophoresis images, Proteomics 4 (8) (2004) 2377–2389.
[14] Å.M. Wheelock, A.R. Buckpitt, Software-induced variance in two-dimensional gel electrophoresis image analysis, Electrophoresis 26 (23) (2005) 4508–4520.
[15] P. Stoica, R.L. Moses, Introduction to Spectral Analysis, Prentice Hall, Upper Saddle River, 1997.
[16] A new false peak elimination method for poor DNA gel images analysis, in: T. RS, N. Jamil, S. Nordin, B. UM (Eds.), Intelligent Systems Design and Applications (ISDA), 2014 14th International Conference on, IEEE, 2014.
[17] D.-C. Tseng, Y.-C. Lee, Automatic band detection on pulsed-field gel electrophoresis images, Pattern. Anal. Applic. 18 (1) (2015) 145–155.
[18] C.K. Chui, An Introduction to Wavelets, Academic Press, 2014.
[19] T. Chai, R. Draxler, Root mean square error (RMSE) or mean absolute error (MAE)? Geosci. Model Dev. Discuss. 7 (2014) 1525–1534.
[20] R. Baeza-Yates, B. Ribeiro-Neto, Modern Information Retrieval, ACM Press, New York, 1999.
[21] L. Montefusco, L. Puccio, Wavelets: Theory, Algorithms, and Applications, Academic Press, 2014.
[22] Z. Liu, A. Abbas, B.-Y. Jing, X. Gao, WaVPeak: picking NMR peaks through wavelet-based smoothing and volume-based filtering, Bioinformatics 28 (7) (2012) 914–920.
[23] W.F.N.Z.C. Yunfei, L.L.M.J.B. Chen, Wavelet denoising and statistical analysis of signal of λ-DNA translocation through nanopores, J. Southeast Univ. (Nat. Sci. Ed.) 1 (2013) 012.
[24] M. Amiri, H. Davandeh, A. Sadeghian, S. Chartier, Feedback associative memory based on a new hybrid model of generalized regression and self-feedback neural networks, Neural Netw. 23 (7) (2010) 892–904.
[25] M. Rafienia, M. Amiri, M. Janmaleki, A. Sadeghian, Application of artificial neural networks in controlled drug delivery systems, Appl. Artif. Intell. 24 (2010) 807–820.
[26] S.M. Hossieni, M. Amiri, S. Najarian, J. Dargahi, Application of artificial neural networks for estimation of tumor parameters in biological tissue, Int. J. Med. Rob. Comput. Assisted Surg. 3 (3) (2007) 235–244 John Wiley & Sons.